ISSN 0018-151X, High Temperature, 2019, Vol. 57, No. 4, pp. 539–546. © Pleiades Publishing, Ltd., 2019.

HEAT AND MASS TRANSFER AND PHYSICAL GASDYNAMICS

Natural Convection in a Square Enclosure with a Conducting Rectangular Shape Positioned at Different Horizontal Locations

Basma Souayeh[a, *], Huda Alfannakh[a], and Manal Al Mutairi[a]

[a]*King Faisal University, College of Science, Physics Department, Alahsa, Saudi, 31982 Arabia*

**e-mail: bsouayeh@kfu.edu.sa*

Received December 2, 2015; revised July 15, 2016; accepted November 8, 2016

Abstract—Numerical simulations are carried out for natural convection in a square enclosure with a conducting horizontal rectangular cylinder. A two-dimensional solution for steady laminar natural convection flow is obtained by using finite-volume method for different Rayleigh numbers varying over the range of 10^3 to 10^6 and using water as the working fluid (Pr = 6.8). The study goes further to investigate the effect of the inner rectangular cylinder position and thermal conductivity ratio on the fluid flow and heat transfer in the cavity. The location of the inner rectangular cylinder is mainly changed horizontally and compared with respect to the vertical case. The effects of Rayleigh numbers, cylinder locations and thermal conductivity on the streamlines, isotherms and average heat transfer of the fluid inside the cavity are investigated. The results indicate that the flow field, temperature distribution, and average rate of the flow field inside the cavity are strongly dependent on the Rayleigh numbers, the position of the inner cylinder, and the thermal conductivity.

DOI: 10.1134/S0018151X19040205

INTRODUCTION

Natural convection in an enclosure is relevant to many industrial applications and tools such as nuclear and chemical reactors, heat exchangers, and cooling of electronic equipment. Natural convection heat transfer exhibits a great variety of complex dynamic behaviors, which depend largely on the geometry and thermal conditions of the enclosure. In some instances, an obstruction may be located somewhere within the enclosure, which could alter the characteristics of flow and heat transfer. Considerable researches have been performed with various heat-conducting obstacles placed inside the enclosure in the form of partitions or partial baffles. However, there is little information about the natural convection processes when a solid heat conducting body is placed within the enclosure and is completely surrounded by the fluid. In applications involving building energy components, such as walls or windows or an electronic equipment, the inserted solid body may reduce the flow, thereby reducing the heat transfer rate across the enclosure; whereas, heat transfer may be enhanced if the solid body has a relatively high thermal conductivity.

For instance, House et al. [1] has studied the effect of a centered conducting body on natural convection in an enclosure. The effects of Rayleigh number, Prandtl number, body size, ratio of thermal conductivities are carried out. The important observation made is that the heat transfer across the enclosure, in comparison to that in the absence of a body, may be enhanced (reduced) by a body with a thermal conductivity ratio less (greater) than unity.

Oh et al. [2] investigated also the steady state heat transfer and flow characteristics of natural convection in a square enclosure containing a conducting heat-generating body. The results show that the flow field and heat transfer are affected by the ratio of the temperature difference across the enclosure to that engendered by the heat source.

This is an important observation as far as conjugate heat transfer is concerned. Sathe et al. [3] studied the natural convection arising from a heat generating substrate-mounted protrusion in an enclosure. The boundaries are maintained at isothermal cold conditions. They concluded that in actual situation, substrate conduction effects cannot be neglected. Also, it may be inappropriate to prescribe simple boundary conditions such as constant temperature or heat flux on the protrusion faces and solve for the governing equations only in the fluid. Furthermore, Sun et al. [4] considered the effect of a heat source and an internal baffle on natural convection heat transfer in a rectangular enclosure. All the walls are of finite conductance. The horizontal walls are considered to be adiabatic on the boundary whereas the vertical walls are differentially heated. They also concluded that it is inappropriate to specify simple boundary conditions on the walls and to neglect the conduction through the baffles. The complete conjugate heat conduction, convection and radiation problem for a heated block in a differentially heated square enclosure is solved by Liu et al. [5]. The boundary conditions of the enclosure are similar to that of de Vahl Davis [6]. In comparison to the problem considered by House et al. [1], the block is generating heat. The conduction and the emission of the block have a substantial effect on the heat transfer situation. Ha et al. [7] conducted a numerical study of conjugate heat transfer of natural

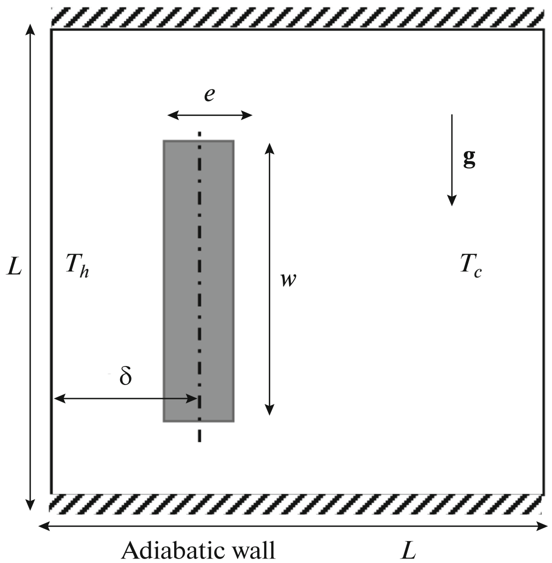

Fig. 1. Schematical configuration of considered model with boundary conditions.

convection in a cubic enclosure with a centered cubic heat-conducting heat generating body. Right and left vertical walls are maintained at differentially heated condition. All other walls are insulated. The presence of the solid body results in a larger variation of the local Nusselt number compared to cases without a cubic conducting body in the enclosure.

Mezrhab et al. [8] studied the radiation-natural convection interactions in a differentially heated square cavity within which a centered, square, heat-conducting body generates heat. For the solution of the governing equations, they have used a specifically developed numerical model based on the finite-volume method and the SIMPLER algorithm. They have found that the isotherms and streamlines are strongly affected by the radiation exchange at high Rayleigh numbers ($\mathrm{Ra} \geq 10^6$). Furthermore, the temperature of the inner body decreases owing the radiation exchange effect. Besides, it was seen that for a fixed Ra, the average Nusselt number at the hot and cold walls ($\mathrm{Nu_h}$ and $\mathrm{Nu_c}$) vary linearly with increasing the temperature difference.

Bilgen [9] studied natural convection in differentially heated square cavities with a thin fin attached on the active wall. The Rayleigh number was varied from 10^4 to 10^9, dimensionless thin fin length from 0.10 to 0.90, dimensionless thin fin position from 0 to 0.90, dimensionless conductivity ratio of thin fin from 0 (perfectly insulating) to 60. Bilgen's [9] results demonstrated that the Nusselt number is an increasing function of Rayleigh number, and a decreasing function of fin length and relative conductivity ratio. It was also found that the heat transfer might be suppressed up to 38% by choosing appropriate thermal and geometrical fin parameters.

Although many researchers have studied the natural convection, there is little information about natural convection processes within a differential square enclosure containing a conducting rectangular obstacle located at different horizontal positions along the center of the enclosure. At this situation, the flow and heat transfer characteristics are largely affected by the location of the conducting body, the Rayleigh numbers and the thermal conductivity ratio. The aim of this study is to examine the effects of the locations of a conducting rectangular body in the enclosure and the conduction on heat transfer and fluid flow, also to investigate the comparison between a horizontal and a vertical location of the conducting shape. The numerical calculations are performed for wide ranges of Rayleigh numbers, the solid-fluid thermal conductivity ratios and inner rectangular cylinder location.

PROBLEM FORMULATION AND GOVERNING EQUATIONS

Physical Model

A concentric conducting rectangular cylinder of height (w) and width (e) located inside a water-filled square cavity with sides of length L is shown in Fig. 1. The left and right side walls are isothermal at the temperatures T_h and T_c, respectively, whereas the bottom and top walls are adiabatic. The rectangular shape moves along the horizontal wall of the cavity in the range from $0.2L$ to $0.8L$. All solid boundaries are assumed to be no-slip rigid walls. Prandtl number is taken to be 6.8, the Rayleigh number is considered in the range 10^3 to 10^6 and the solid-fluid thermal conductivity ratios are taken as 0.1, 1 and 50. All fluid properties are assumed to be constant except for the density variation in the buoyancy term which is treated according the Boussinesq approximation. The radiation effects are neglected and the gravitational acceleration acts in the negative y-direction. The fluid within the enclosure is assumed incompressible and Newtonian while viscous dissipation effects are considered negligible. The flow and thermal fields inside the square enclosure with a conducting rectangular body are described by the Navier-Stokes and the energy equations, respectively.

Non-dimensional Equations

The governing equations are transformed into a dimensionless form under the following non-dimensional variables.

The dimensionless variables in the above equations were defined as

$$t = \frac{t^*\alpha_f}{L^2},\quad x = \frac{x^*}{L},\quad y = \frac{y^*}{L},\quad v = \frac{v^*L}{\alpha_f},\quad u = \frac{u^*L}{\alpha_f},$$
$$p = \frac{p^*L^2}{\rho_f\alpha_f^2},\quad \alpha = \frac{\alpha_s}{\alpha_f},\quad \theta = \frac{T - T_c}{T_h - T_c}. \tag{1}$$

The dimensionless forms of the governing equations under steady state condition are expressed in the following forms:

$$\frac{\partial u}{\partial x}+\frac{\partial v}{\partial y}=0, \quad (2)$$

$$\frac{\partial u}{\partial t}+u\frac{\partial u}{\partial x}+v\frac{\partial u}{\partial y}=-\frac{\partial p}{\partial x}+\sqrt{\frac{\mathrm{Pr}}{\mathrm{Ra}}}\left(\frac{\partial^2 u}{\partial x^2}+\frac{\partial^2 u}{\partial y^2}\right), \quad (3)$$

$$\frac{\partial v}{\partial t}+u\frac{\partial v}{\partial x}+v\frac{\partial v}{\partial y}=-\frac{\partial p}{\partial y}+\sqrt{\frac{\mathrm{Pr}}{\mathrm{Ra}}}\left(\frac{\partial^2 v}{\partial x^2}+\frac{\partial^2 v}{\partial y^2}\right)+\theta, \quad (4)$$

$$\frac{\partial \theta_f}{\partial t}+u\frac{\partial \theta_f}{\partial x}+v\frac{\partial \theta_f}{\partial y}=\frac{1}{\sqrt{\mathrm{RaPr}}}\left(\frac{\partial^2 \theta_f}{\partial x^2}+\frac{\partial^2 \theta_f}{\partial y^2}\right), \quad (5)$$

$$\frac{\partial \theta_s}{\partial t}=\frac{\alpha}{\sqrt{\mathrm{RaPr}}}\left(\frac{\partial^2 \theta_s}{\partial x^2}+\frac{\partial^2 \theta_s}{\partial y^2}\right). \quad (6)$$

In the above equations ρ, T, α_s, and α_f represent the density, dimensional temperature, thermal diffusivity of solid and fluid, respectively. The superscript * in Eq. (1) represents the dimensional variables u_i, p, t, θ, and α are the non-dimensional velocity, pressure, time, temperature and thermal diffusivity. The above non-dimensional results in two dimensionless parameters:

$$\mathrm{Pr}=\frac{\nu}{\alpha_f}, \quad \mathrm{Ra}=\frac{g\beta L^3(T_h-T_c)}{\nu\alpha_f},$$

where ν, g, and β are the kinematic viscosity, gravitational acceleration and volume expansion coefficient. For the boundary conditions, the velocities are set to zero for all solid walls. The temperature boundary conditions and the conditions at the fluid/body interfaces are as follows:

$$\text{at } x=0, \quad \theta=1,$$

$$\text{at } x=1, \quad \theta=0,$$

$$\text{at } y=0 \text{ and } 1,$$

$$\frac{\partial \theta}{\partial x}=0.$$

At fluid/body interface and $\theta_s=\theta$

$$\frac{\partial \theta}{\partial n}=k\frac{\partial \theta_s}{\partial n},$$

where $k=k_s/k_f$ is thermal conductivities ratio of conducting solid body to fluid.

Physical quantities of interest in this problem is the mean Nusselt number which can be expressed as:

$$\overline{\mathrm{Nu}}=\frac{1}{L}\int_0^L \mathrm{Nu}ds. \quad (7)$$

NUMERICAL METHODOLOGY

Solution Method

Equations (2)–(6) subject to the boundary conditions of the present study were integrated using the finite-volume method and an iterative successive-over-relaxation scheme [10] with multigrid acceleration. The main idea of multigrid methods can be found in [11]. If specific details about the computational methodology are needed, the reader is directed to Ben Cheikh et al. [12]. The convergence criterion is the maximal residual of all the governing equations which is less than 10^{-6}. In addition to the usual accuracy control, the accuracy of computations is also controlled using the energy conservation within the system.

Table 1. Results of grid independence tests in a square cavity incorporating a Conducting body located at $\delta = 0.5$ with $\mathrm{Pr} = 6.8$, $\mathrm{Ra} = 10^5$, and $k = 0.1$

Grid	$\overline{\mathrm{Nu}}$	ψ_{max}	ψ_{min}
24 × 24	4.493	19.421	19.176
48 × 48	4.537	19.239	18.960
	(0.969%)	(0.937%)	(1.126%)
96 × 96	4.555	19.224	18.905
	(0.395%)	(0.077%)	(0.290%)
192 × 192	4.550	19.176	18.875
	(0.043%)	(0.249%)	(0.158%)

Grid Independency Study

Results of grid dependency tests through the surface average Nusselt number and streamline function of the conducting body when $\mathrm{Ra} = 10^5$, $\mathrm{Pr} = 6.8$, $k = 0.1$, and $\delta = 0.5$ are regrouped in Table 1 for four different non-uniform grids namely: 24, 48, 96 and 192. In the present study, independence of numerical results from the mesh size was assumed when the difference in the simulated values computed between two consecutive grids was less than 1%. As it can be observed from the deviation values reported in Table 1, a non-uniform grid of 96 × 96 is sufficiently fine to ensure the grid.

Validation of the Code

Extensive validation of the developed code has been carried out by comparing the results of a Rayleigh-Bénard convection square filled with a square conducting body in the center of the layer with those of Lee et al. [13]. The average Nusselt number through the hot wall has been computed for different thermal conductivity ratio $k = 0.1$, 1, and 50. The same has been performed for $\mathrm{Ra} = 10^3$, 10^4, 10^5, and 10^6 and a Prandtl number 0.71 corresponding to that of air are shown in Table 2. Excellent agreement has been obtained.

RESULTS AND DISCUSSION

Combined Effects of Thermal Conductivity, Rayleigh Number, and Location of the Inner Body on the Flow

The basic features of the flow and thermal fields in a square enclosure of same height and width, with a conducting rectangular solid cylinder of $0.6L$ (height) and $0.2L$ (width) are plotted for an horizontal position

Table 2. Values of average Nusselt number on the hot wall with those from [13] according to the cavity with conducting body

K	$k = 0.1$			$k = 1$			$k = 50$		
Ra	present study	[13]	error, %	present study	[13]	error, %	present study	[13]	error, %
10^3	0.81	0.81	0.00	1.00	1.00	0.00	1.27	1.27	0.00
10^4	2.31	2.31	0.00	2.12	2.13	0.46	1.59	1.56	1.92
10^5	3.85	3.85	0.00	3.86	3.88	0.51	3.93	3.94	0.52
10^6	6.18	6.30	1.90	6.19	6.29	1.58	6.20	6.31	1.74

for the Rayleigh number in the range of 10^3–10^6 and for a solid-fluid thermal conductivity ratios (k) values of 0.1, 1 and 50. The Prandtl number of the fluid considered is 6.8 (water).

Figure 2 shows isotherms and streamlines in the enclosure for different Rayleigh numbers with heat-conducting body at $k = 0.1$ and a thermal diffusivity $\alpha = 0.001$ for inner rectangular cylinder location taken as 0.2 and 0.5. In fact, we are limited just to these location values because there is a real symmetry in results against the center of the cavity and a similarity between plots of $\delta = 0.2$, 0.3 and $\delta = 0.4$, 0.5.

At low values of Ra, the heat transfer in the enclosure is predominantly due to conduction. When $k = 0.1$, the thermal conductivity of fluid is ten times higher than that of conducting body and as a result the distribution of isotherms at $k = 0.1$ appear to be nearly parallel to the active walls and concentrated near the conducting block for the four rectangular cylinder location considered.

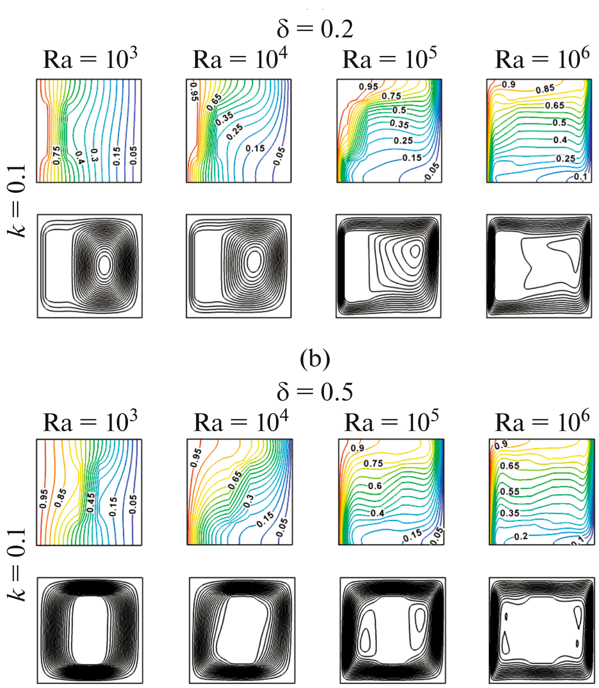

Fig. 2. Distribution of isotherms (top) and streamlines (bottom) for the conducting body at $k = 0.1$ and $\alpha = 0.001$ for two horizontal locations (a)–(b).

When Rayleigh number increases, the flow velocity increases and it causes a stronger circulation near the hot and cold walls. If the Rayleigh number is increased to 10^5, the thickness of the thermal layer formed on the side walls becomes thinner due to the flow acceleration and the gradient of thermal boundary layer becomes larger, meaning that the heat transfer rate increases with increasing Rayleigh number, isotherms are stratified in the center of the cavity and tightened at the active walls specifically in the upper corner of the cold wall and the bottom corner of the hot wall. Besides, the isotherms move in the direction of clockwise and become almost horizontal in the inner body especially in the center of the cavity. When the isotherms are stratified horizontally across the cavity, boundary layers are intensifying across the hot and cold wall, so we notice that the Rayleigh number increases to 10^5 and 10^6, the effect of convection on the fluid flow and heat transfer in the enclosure increases and become more dominant than conduction. These observations are considered valid for all selected positions of the conducting shape $\delta = 0.2$ and 0.5 in the cavity, which means that position has no effect on the temperature fields.

As regards the thermal conductivity ratio $k = 1$ which correspond a thermal diffusivity $\alpha = 1$, the distribution of the temperature in the enclosure is given by isotherms in Fig. 3. As we can see, the isotherms show a high thermal gradient at the vertical walls and a net stratification of temperatures in the center. By increasing the Rayleigh number (Ra), isotherms become constricted near the active walls and the phenomena of the stratification of the temperatures are more pronounced especially in the center of the cavity.

Figure 4 shows isotherms in the enclosure for different Rayleigh numbers with heat-conducting body at $k = 50$ and $\alpha = 0.05$. When $k = 50$, a thermal conductivity of fluid is 50 times less than solid thermal conductivity. Because a heat-conducting body conducts more heat through the body, as aforementioned, when $k = 0.1$, the thermal conductivity of conducting body is very smaller than the fluid. Thus the temperature in the conducting body is not uniform and has a large gradient. However, the temperature in the conducting body for the case of $k = 50$ is almost uniform due to large thermal conductivity of conducting body. As a result, when Ra = 10^3 and 10^4 at which the conduction is the dominant heat transfer mode, the tem-

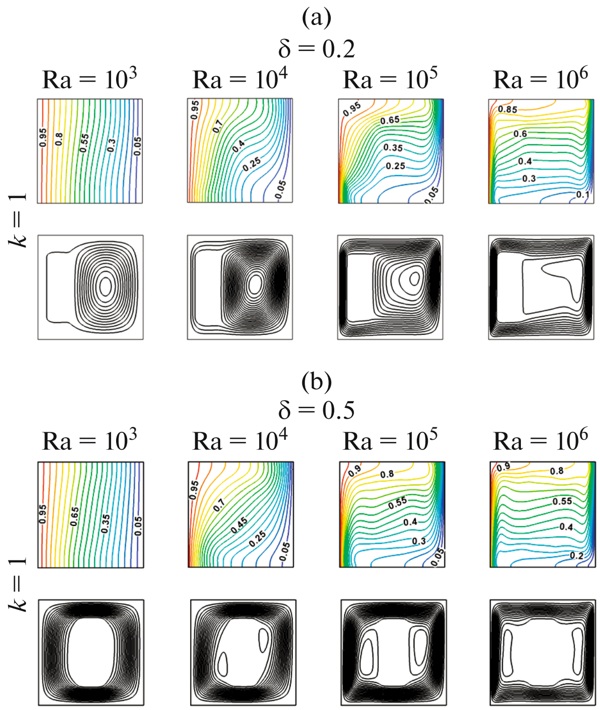

Fig. 3. Distribution of isotherms (top) and streamlines (bottom) for the conducting body at $k = 1$ and $\alpha = 1$ for two horizontal locations (a)–(b).

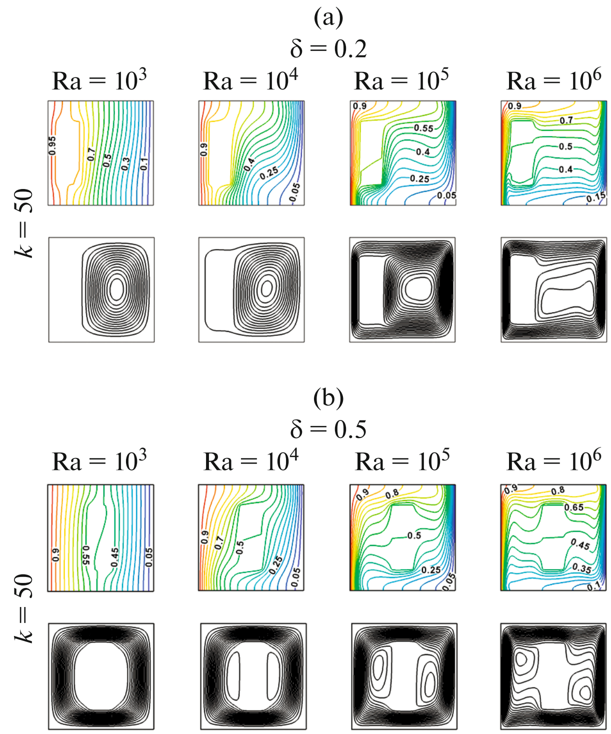

Fig. 4. Distribution of isotherms (top) and streamlines (bottom) for the conducting body at $k = 50$ and $\alpha = 0.05$ for two horizontal locations (a)–(b).

perature fields for the case of $k = 50$ have different distribution from those for the case of $k = 0.1$ and $k = 1$. Especially differences in the inside of the enclosure and around the conducting body are large. When the Rayleigh number increases to 10^5 and 10^6, the thermal resistance for conduction in the conducting body does not change but the thermal resistance for convection in the fluid decreases with increasing convective heat transfer. Thus, when $\text{Ra} = 10^5$ and 10^6, the distribution of isotherms for $k = 50$ is similar to that for $k = 0.1$, except for the slight difference in and close to the conducting body.

Concerning streamlines for the lowest value of Rayleigh number and for the same conducting body locations, the fluid flow circulating in the clockwise direction around a conducting body is forming a single eddy emerges occupying the whole volume of the enclosure with the center of recirculation positioned approximately near the center of the cavity and that stretches to the cold wall at higher values of Ra. As Ra is increasing, streamline patterns show regions of flow separation. We note therefore that the position of the conductive body does not affect the isotherms and a very slight variation on the streamlines occur especially for small Rayleigh numbers, where the eddies in the center of the cavity are significant for small Rayleigh numbers (10^3–10^4) at 0.2 then disappear when $\text{Ra} = 10^6$ at $\delta = 0.5$. The flow fields for the case of $k = 50$ are generally similar to those for the cases of $k = 0.1$ and $k = 1$.

Effects of Governing Parameters on Heat Transfer Rate

For $\text{Ra} = 10^3$, we may note that the variations profiles of average Nusselt number versus the position corresponding to the three values of the thermal conductivity ratio $k = 0.1$, $k = 1$ and $k = 50$ are almost flat and symmetrical with respect to median plane of the cavity at $\delta = 0.5$ that is to say that the position has no effect on the heat transfer rate for the same Rayleigh number and the different conductivity of reports considered. In contrast, the conductivity ratio of the solid relative to the fluid has significant effect because more than k increases more the average Nusselt number

Table 3. Comparison of average Nusselt numbers for different locations for $\text{Pr} = 6.8$, $k = 0.1$, and $\text{Ra} = 10^5$

Ra	$\delta = 0.2$	$\delta = 0.3$	$\delta = 0.4$	$\delta = 0.5$	$\delta = 0.6$	$\delta = 0.7$	$\delta = 0.8$
10^5 (horizontal locations)	3.558	4.589	4.560	4.555	4.560	4.589	3.558
10^5 (vertical locations)	3.966	4.653	4.806	4.830	4.806	4.652	3.966

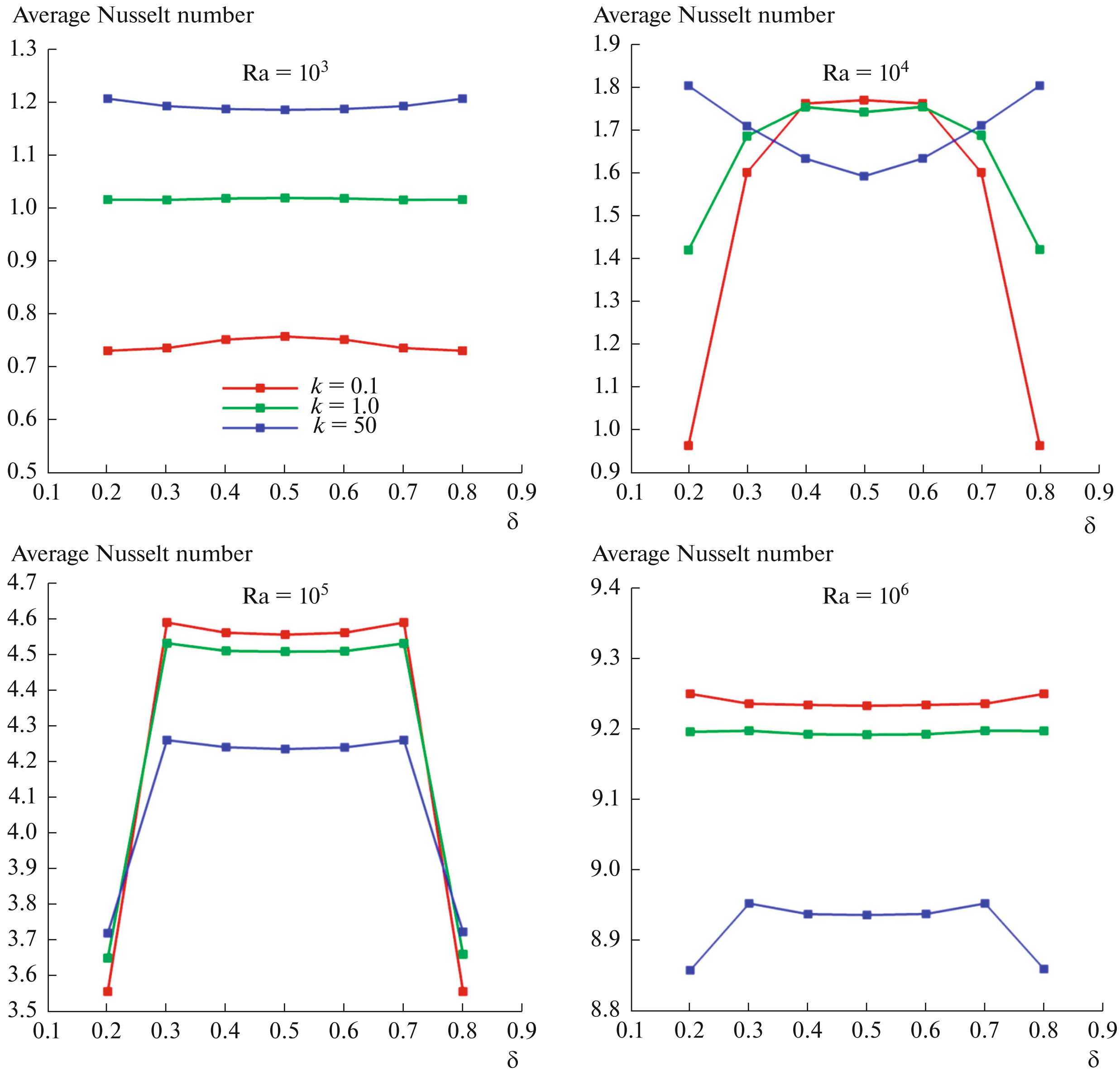

Fig. 5. The effect of δ on average Nusselt number for different Rayleigh numbers and thermal conductivity ratios k.

increases. Similarly, for $\mathrm{Ra} = 10^4$, the symmetry about the median plane is also exhibited. It is also noted that the position of the conductive body has a significant effect on the average heat transfer rate. For $k = 0.1$, we may see that average heat transfer rate increases until a maximum value at $\delta = 0.5$ after which it decreases. For $k = 1$, the same phenomena happens but for both maximum $\delta = 0.4$ and $\delta = 0.6$ At the value $k = 50$, the opposite phenomenon occurs which means that the heat transfer lowers with respect to the position of the solid conductor until reaching a minimum value $\delta = 0.5$ and then increases again. At the value $\mathrm{Ra} = 10^5$, a symmetry with respect to the center of the cavity ($\delta = 0.5$) is always present, the average heat transfer rate strengthens between the positions of the conductive body in the cavity $\delta = 0.2$ and $\delta = 0.3$. Then, at the positions of the solid conductor between 0.3 and 0.7, the average heat transfer is almost steady after which it decreases again. Another gradual decrease is seen again passing from $\delta = 0.7$ to $\delta = 0.8$. We also note that the heat transfer means varies disproportionately compared to conductivity ratio k. Finally for $\mathrm{Ra} = 10^6$, still a marked symmetry is observed with respect to the middle of the square cavity. It also noted that the average heat transfer decreases with the conductivity ratio of the solid with respect to the fluid. For $k = 0.1$ and $k = 1$, the average heat transfer is almost constant that is to say the position of the solid conductor has no effect on this transfer while for $k = 50$ and δ between 0.2 and 0.3 the average heat transfer augments significantly, returns to be stable between

0.3 and 0.7 and then decreases passing from the position 0.7 to 0.8.

So we conclude that Fig. 5 showing the variation of average Nusselt number as a function of the horizontal locations of the conducting body for various Rayleigh numbers with $k = 0.1$, 1 and 50, proves that for Ra = 10^3, average Nusselt number remains constant for the range ofconsidered indicating that conductionis the dominant mode of heat transfer. Therefore, when Ra rises until reaching 10^6, the increase of δ generates a significant increase in the average Nusselt number and this is due to the convection, which is the dominant mode of heat transfer.

By analyzing the variations of the average heat transfer for the Rayleigh number between 10^3 and 10^6 through the two vertical walls of the cavity and according to the positions of the treated solid conductor ($0.2 \le \delta \le 0.8$) and for the thermal conductivity ratio of reports studied: $k = 0.1$, 1 and 50, we can see that for a definite position of the solid conductor and a fixed ratio conductivity, heat transfer rate increases with the Rayleigh number. However, this transfer rate increases in generally with the thermal conductivity ratio for the same Rayleigh number with some exceptions, and for a fixed position of the conductive body. Quantitatively, concerning the conductivity ratio $k = 0.1$, it is observed that for small Rayleigh numbers (10^3–10^4), the heat transfer is optimal for a position of the solid conductor $\delta = 0.5$, this finding is more approved in Fig. 5. However, for large Rayleigh numbers (Ra = 10^5), the heat transfer is maximal when the solid conductor is close to the active walls. By further increasing the Rayleigh number up to 10^6, this transfer is more enhanced by approaching more the two vertical walls: $\delta = 0.2$ and $\delta = 0.8$. According to the conductivity ratio $k = 50$, it is seen that the phenomena observed in $k = 0.1$ and $k = 1$ are inverted that is to say that the heat transfer is optimal near the active walls and small Rayleigh numbers 10^3–10^4, but increasing this number to reach 10^5–10^6, the heat transfer is maximal by further moving away from the two hot and cold vertical walls.

In the realm of thermal engineering applications, the overall effectiveness of heat transfer is unquestionably the most relevant parameter. For this purpose, the average Nusselt number Nu defined in Eq. (7) is graphed versus Ra in Fig. 6 for the four horizontal locations of the conducting body and the considered thermal conductivity ratio: $k = 0.1$, $k = 1$ and $k = 50$. It can be confirmed that Nu is almost invariant and close to unity whenever Ra $\le 10^4$ for all selected locations of the conducting shape and dimensionless thermal conductivity; this is means that the heat transfer mechanism is almost due to convection. At Rayleigh numbers Ra higher than 10^4, the average heat transfer increases significantly due to enhanced natural convection. Finally, the numerical results obtained for the average Nu in conjunction with the

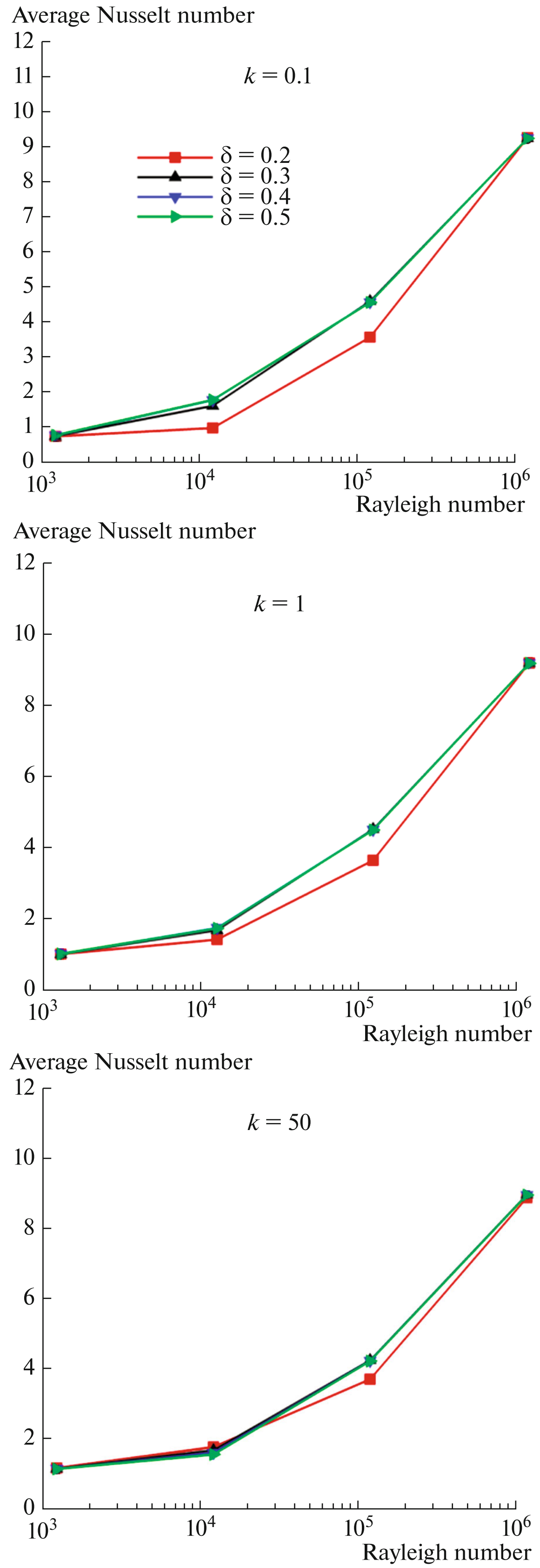

Fig. 6. Average Nusselt number as function of Ra for various thermal conductivity ratios *k*.

different Ra have been post processed for $10^3 \leq \text{Ra} \leq 10^6$. From these figures, it can be observed that no significant effect are observed of solid-fluid thermal conductivity ratios (k) on the average Nusselt number values.

Comparison of Different Location Results

From Table 3 and for a fixed Rayleigh number $\text{Ra} = 10^5$ and a solid-fluid thermal conductivity ratios $k = 0.1$ and for the same rectangular-shaped conducting body which is positioned vertically in this case and in the same locations chosen when it was positioned vertically, it can be seen that average Nusselt numbers are greater than the corresponding values when the rectangular cylinder is positioned horizontally for the selected values of (δ). Moreover, in this case the average Nusselt number values are increasing gradually until ($\delta = 0.5$), then we observe a symmetric behavior against the mid-cavity.

CONCLUSIONS

Natural convection in a differentially heated enclosure filled with water containing a rectangular conducting body, was successfully solved numerically. We made a detailed analysis for the distribution of streamlines, isotherms, and Nusselt number in order to investigate the effect of the locations and the presence of a conducting body with different thermal conductivity ratios of $k = 0.1$, 1, and 50 on the fluid flow and heat transfer in the horizontal enclosure for the Rayleigh numbers in the range of $10^3 \leq \text{Ra} \leq 10^6$. Comparison between horizontal and vertical locations of the conducting shape in the enclosure was made.

The results demonstrate that for a fixed solid–fluid thermal conductivity ratios (k), the position of the conductive body (δ) does not affect the isotherms and a very slight variation on the streamlines occur especially for small Rayleigh numbers, also the thermal boundary layers near the hot and cold sides increase and concentrate as the Rayleigh number increases.

For low values of Rayleigh numbers, average Nusselt number remains constant for the range of δ considered indicating that conduction is the dominant mode of heat transfer. Therefore, when Ra rises until reaching 10^6, the increase in δ generates a significant increase in the average Nusselt number and this is due to the convection, which is the dominant mode of heat transfer.

The average heat transfer for the Rayleigh number between 10^3 and 10^6 through the two vertical walls of the cavity and according to the positions of the treated solid conductor ($0.2 \leq \delta \leq 0.8$) and for the thermal conductivity ratio $k = 0.1$, 1, and 50 was studied. We can see that for a definite position of the solid conductor and a fixed ratio conductivity, heat transfer rate increases with the Rayleigh number. However, this transfer rate increases generally with the thermal conductivity ratio for the same Rayleigh number with some exceptions, and for a fixed position of the conductive body.

For a fixed Rayleigh number $\text{Ra} = 10^5$ and a solid–fluid thermal conductivity ratio $k = 0.1$ and for the same rectangular-shaped conducting body, it can be seen that when the conducting solid is positioned vertically the average Nusselt numbers are greater than the corresponding values when it is positioned horizontally for the selected values of δ. Moreover, in this case the average Nusselt number values are increasing gradually until $\delta = 0.5$, then we observe a symmetric behavior against the mid-cavity.

REFERENCES

1. House, J.M., Beckerman, C., and Smith, T.F., *Numer. Heat Transfer, Part A*, 1990, vol. 18, p. 213.
2. Oh, J.Y., Ha, M.Y., and Kim, K.C., *Numer. Heat Transfer*, 1997, vol. 31, p. 289.
3. Sathe, S.B. and Joshi, Y., *Int. J. Heat Mass Transfer*, 1991, vol. 34, p. 2149.
4. Sun, Y.S. and Amery, A.F., *Int. J. Heat Mass Transfer*, 1997, vol. 40, p. 915.
5. Liu, Y. and Thien, N.P., *Comput. Mech.*, 1999, vol. 24, p. 175.
6. de Vahl Davis, G., *Int. J. Numer. Methods Fluids*, 1983, vol. 3, p. 249.
7. Ha, M.Y. and Jung, M.J., *Int. J. Heat Mass Transfer*, 2000, vol. 43, p. 4229.
8. Bouzidi, M., Firdaouss, M., and Lallemand, P., *Phys. Fluids*, 2001, vol. 13, p. 3452.
9. Bilgen, E., *Int. J. Heat Mass Transfer*, 2005, vol. 48, p. 3493.
10. Barrett, R., et al., *Templates for the Solution of Linear Systems: Building Blocks for Iterative Methods*, Soc. Ind. Appl. Math., 1994.
11. Hackbusch, W., *Multi-Grid Methods and Applications*, Springer, 1985.
12. Ben-Cheikh, N., Ben-Beya, B., and Lili, T., *C. R. Mec.*, 2007, vol. 335, p. 113.
13. Lee, J.R. and Ha, M.Y., *Int. J. Heat Mass Transfer*, 2005, vol. 48, p. 3308.